International Journal on
"Technical and Physical Problems of Engineering"
(IJTPE)
Published by International Organization of IOTPE

ISSN 2077-3528
IJTPE Journal
www.iotpe.com
ijtpe@iotpe.com

December 2024 | Issue 61 | Volume 16 | Number 4 | Pages 283-292

COMPUTATIONAL INVESTIGATION OF TURBULENCE NEAR AIRFOIL BOUNDARY LAYERS

S. El Ouardi [1] B. Radi [2] R. El Maani [3] J. Smily [2] L. Zahiri [1] K. Mansouri [1]

1. Laboratory of Modeling and Simulation of Intelligent Industrial Systems, Higher Normal School of Technical Education, Hassan II University, Mohammedia, Morocco
so.elouardi@uhp.ac.ma, zahiri@enset-media.ac.ma, khalifa.mansouri@enset-media.ac.ma
2. Laboratory of Engineering, Industrial Management and Innovation, Hassan I University, Settat, Morocco
bouchaib.radi@yahoo.fr, jaouadsmily@gmail.com
3. Laboratory of Computer and Mathematical Process Engineering, Sultan Moulay Slimane University, Khouribga, Morocco, elmaani.rabi3@gmail.com

Abstract- Turbulence in aerodynamics, characterized by irregular and chaotic airflows, poses critical challenges for optimizing aircraft performance and ensuring operational safety. This study addresses these challenges by exploring advanced turbulence modeling techniques for the analysis of transonic compressible flows around a NACA 0012 airfoil profile. Using computational fluid dynamics tools within FLUENT, a hybrid simulation framework is implemented, combining DES and LES in freestream regions, with RANS modeling near the wall. The DES model is validated against experimental data, demonstrating high accuracy and efficiency in capturing turbulence effects while significantly reducing mesh density. Additionally, the Smagorinsky subgrid-scale model applied in LES effectively resolves fine-scale vortices near the airfoil surface, although it requires increased computational resources due to higher mesh resolution demands. These findings highlight the potential of hybrid turbulence modeling approaches to improve the predictive capabilities of aerodynamic simulations. The study provides a robust framework for enhancing turbulence analysis in complex aerodynamic environments, offering valuable insights for optimizing airfoil design and advancing aerodynamic performance evaluation techniques.

Keywords: CFD, Aerodynamic, NACA Profile, Turbulence, LES, DES, RANS.

1. INTRODUCTION

The development and refinement of Computational Fluid Dynamics (CFD) have been driven by the ongoing need to reduce computational time while maintaining high accuracy through robust methods [1]. In fields such as aerospace, automotive, and industrial engineering, where fluid interactions are crucial, CFD remains a preferred and indispensable tool for design, analysis, and performance optimization [2]. The importance of turbulence theories in CFD cannot be overstated, as accurately modeling turbulence is fundamental to predicting airflow behaviors, lift, drag forces, and overall aerodynamic efficiency. A thorough understanding of turbulence modeling not only improves simulation reliability but also aids in reducing costs and computational effort.

Turbulence, characterized by chaotic and irregular fluid motion, poses a significant challenge in aerodynamic studies. In applications such as aircraft wing design and engine cooling, precise turbulence modeling ensures better performance and operational safety. Dorri et al. [3] illustrated this concept by studying heat transfer performance in an air-cooled motorcycle engine with varying fin geometries. Their research demonstrated how the interaction of airflow and fin shape significantly influences thermal performance, highlighting the critical role of turbulence models in accurately simulating such interactions.

Many commercial CFD tools facilitate the analysis of airflow around objects in fluid mechanics, allowing engineers to visualize and understand characteristics that are difficult, costly, or impossible to measure experimentally. Accurate turbulence modeling in these simulations, which covers both local interactions and global flow patterns, is essential to capture performance indicators such as lift and drag forces [5]. Typically, CFD projects begin by setting modeling objectives and creating the geometry, followed by mesh generation. Here, designers strike a balance between computational cost and accuracy by selecting appropriate mesh density and resolution [1]. The solver then processes these equations, and appropriate physical models are integrated to calculate and analyze the results.

Turbulence theories, such as Reynolds-Averaged Navier-Stokes (RANS) equations [9], play a crucial role in CFD simulations. Reynolds [10] proposed breaking instantaneous flow quantities into time-averaged and fluctuating components, allowing approximate but computationally efficient solutions.

Registered: 240604 | Article Info: 1924 | Accepted: 241128
Reserved: 241016 | Available: 241231

Despite their computational efficiency, RANS models may not capture transient details as accurately as more sophisticated models like Detached Eddy Simulations (DES) or Large Eddy Simulations (LES). Comparatively, RANS models offer the lowest computational cost and are widely applicable for steady-state flows at moderate Reynolds numbers. However, their accuracy diminishes in cases involving significant flow separation or unsteady phenomena. LES models, on the other hand, resolve large-scale turbulent structures directly, providing unparalleled accuracy for high Reynolds number flows but at the cost of significantly higher computational resources. DES bridges the gap between RANS and LES by combining the stability of RANS near solid boundaries with the precision of LES in separated regions, making it particularly suitable for transonic flows and high-Reynolds-number applications. The choice of model often depends on the desired balance between accuracy and computational efficiency, as well as the specific flow regime (e.g., low versus high Mach numbers).

The aerodynamic interactions of aircraft wings with airflow have been a significant area of research, as highlighted by Ashley and Rodden [8]. In this context, Schmidt and Thiele [13] applied DES models to simulate airflow around 2D and 3D airfoils, capturing time-varying boundary layer developments and transient flow dynamics. Jones [11, 12] further advanced our understanding by examining airflow behavior over the NACA 0012 airfoil at low Reynolds numbers, revealing the effects of airfoil incidence changes on the separation bubble dynamics.

Recent advances in wind energy applications also demonstrate the significance of turbulence modeling. Garcia, et al. [4] focused on optimizing wind turbine blade design to maximize energy output, emphasizing the role of aerodynamic interactions in wind energy efficiency. Machine learning approaches, as proposed by Zhu, et al. [14], offer new methods for turbulence modeling by mapping turbulent viscosity to flow variables, enhancing predictive accuracy in subsonic flows. Particle Swarm Optimization (PSO) techniques, presented by Echavarri, et al. [6], provide robust solutions for tuning small wind turbine pitch control systems, which are critical for maximizing energy capture efficiency. Nayir, et al. [7] also highlighted new trends in wind turbine control and wind energy modeling, addressing the challenges of grid integration and system efficiency.

Moreover, the one-equation turbulence model introduced by Apalart and Allmaras [15] remains a practical choice for simplifying and accelerating aerodynamic simulations without compromising essential performance metrics. This model strikes a balance between computational efficiency and the fidelity required for accurate aerodynamic predictions. This study aims to evaluate and compare the performance of various turbulence models (RANS, DES, and LES) by analyzing the turbulent fluid flow around a NACA 0012 airfoil in a transonic regime. A validated methodology is developed by comparing simulation results with experimental data available in the NASA database, ensuring the models' accuracy while integrating insights from contemporary turbulence theories and CFD research. The findings of this study contribute to enhancing aerodynamic modeling strategies, improving prediction accuracy, and offering practical guidance for selecting optimal turbulence models in CFD simulations for complex aerodynamic environments.

2. THEORETICAL FORMULATION OF TURBULENCE MODELING APPROACHES

2.1. Turbulence Modeling Using LES

The LES approach stands as a prominent method in computational fluid dynamics, offering a sophisticated means to model turbulent flows. In LES, the focus is on resolving the large-scale eddies explicitly, while the smaller-scale eddies are incorporated implicitly using subgrid-scale models [15]. This approach has gained significance in the study of complex aerodynamic interactions, providing valuable insights into phenomena such as separation bubbles and vortex dynamics. In this exploration, we delve into the principles and applications of the LES approach, examining its efficacy in capturing turbulent behaviors and enhancing our understanding of fluid dynamics. The velocity field in this model has been mathematically divided in two parts, one is resolved and it presents the large eddies and the other in the form of a sub-grid which presents the small eddies whose SGS model includes the effect of the captured part:

$$\bar{u}_i(\vec{x}) = \int u(\vec{\xi}) G\left(\vec{x} - \vec{\xi}\right) d\vec{\xi} \tag{1}$$

with:

$$u_j \frac{\partial u_i}{\partial x_j} + \frac{\partial u_i}{\partial t} = \frac{\partial}{\partial x_j}\left(\nu \frac{\partial u_i}{\partial x_j}\right) - \frac{1}{\rho}\frac{\partial p}{\partial x_i} \tag{2}$$

The appropriate fraction of the tension tensor assigned to the sub grid size model is represented by u_i'. Where, $\bar{u}_i$ is the portion of the strain rate tensor associated with the resolvable scale. This part is mainly focused on incompressible flow. Favre's approximation is used for compressible flows. The equations of fluid motion are:

$$\bar{u}_j \frac{\partial \bar{u}_i}{\partial x_j} + \frac{\partial \bar{u}_i}{\partial t} = \frac{1}{\rho}\frac{\partial \tau_{ij}}{\partial x_j} - \frac{1}{\rho}\frac{\partial \bar{p}}{\partial x_i} + \frac{\partial}{\partial x_j}\left(\nu \frac{\partial \bar{u}_i}{\partial x_j}\right) \tag{3}$$

The processes of differencing and filtering can be interchanged. Although filters have been constructed that switch the differencing, the errors introduced by this assumption are considered minimal. The term $\frac{\partial \tau_{ij}}{\partial x_j}$ due to the nonlinear transport terms, in view of:

$$\bar{u}_j \frac{\partial \bar{u}_i}{\partial x_j} \neq \frac{\partial \bar{u}_i}{\partial x_j} \bar{u}_j \tag{4}$$

where:

$$\tau_{ij} = \bar{u}_i \bar{u}_{ij} - \bar{u}_i \bar{u}_j \tag{5}$$

The Boussinesq hypothesis is used in small-scale turbulence models, The deviatoric part of the subgrid-scale stress tensor is formulated as:

$$\tau_{ij} - \frac{1}{3}\delta_{ij}\tau_{kk} = -2\overline{S}_{ij} \tag{6}$$

where, $\overline{S}_{ij}$ is the tensor representing the strain rate at the resolved scales can be described as follows:

$$\overline{S}_{ij} = \frac{1}{2}\left(\frac{\partial \overline{u}_i}{\partial x_j} + \frac{\partial \overline{u}_j}{\partial x_i}\right) \tag{7}$$

where, ν_t is turbulent viscosity. By performing filtering operation on the Navier-Stokes equations, the result is:

$$\frac{\partial \overline{u}_i}{\partial t} + \overline{u}_j \frac{\partial \overline{u}_i}{\partial x_j} = -\frac{1}{\rho}\frac{\partial \overline{p}}{\partial x_i} + \frac{\partial}{\partial x_j}\left(\left[\nu + \nu_t\right]\frac{\partial \overline{u}_i}{\partial x_j}\right) \tag{8}$$

The incompressibility condition is applied to simplify the equation, with the pressure modified to incorporate the diagonal term $\tau_{kk}\delta_{ij}/3$. The essence of the Smagorinsky model can be encapsulated in the following manner:

$$\tau_{ij} - \frac{1}{3}\tau_{kk}\delta_{ij} = -2\left|\overline{S}\right| S_{ij}\left(C_S\Delta\right)^2 \tag{9}$$

The equation for eddy viscosity in the context of the Smagorinsky-Lilly model [9] is expressed as follows:

$$\mu_{sgs} = \rho\left(C_s\Delta\right)^2\left|\overline{S}\right| \tag{10}$$

The dimension of the filter is typically considered as:

$$\Delta = \left(Volume\right)^{\frac{1}{3}} \tag{11}$$

The calculation of the eddy viscosity is based on:

$$\mu_{eddy} = \mu_{mol} + \mu_{sgs} \tag{12}$$

The typical value assigned to the Smagorinsky constant is:

$$C_s = 0.1 \sim 0.2 \tag{13}$$

2.2. Turbulence Modeling Using RANS

The RANS is a method to simulate vortices. A number of statistical models, or unstable Navier-Stokes equations, have been modified through the introduction of two types of quantities: an average and a fluctuating quantity that is derived from utilizing the Reynolds average. This allows the models to accurately depict the effects of turbulence and, in the end, has the Navier-Stokes equations averaged by Reynolds [16]. To derive the turbulence model equations from RANS, a statistical averaging approach is employed; thus, the models are referred to as statistical models. In Einstein notation, these equations may be expressed as follows:

$$\rho\overline{u}_j\frac{\partial \overline{u}_i}{\partial x_j} = \rho\overline{f}_i + \frac{\partial}{\partial x_j}\left[-\overline{p}\delta_{ij} + \mu\left(\frac{\partial \overline{u}_i}{\partial x_j} + \frac{\partial \overline{u}_j}{\partial x_i}\right) - \rho u_j' u_i'\right] \tag{14}$$

where, $\left(-\rho\overline{u}_j'\overline{u}_i'\right)$ denotes Reynold's stress, the governing equations of Reynolds-averaged flow is as follows:

$$\frac{\partial\left(\rho u_i\right)}{\partial x_i} + \frac{\partial \rho}{\partial \rho} = 0 \tag{15}$$

$$\frac{\partial\left(\rho u_i u_j\right)}{\partial x_j} + \frac{\partial\left(\rho u_i\right)}{\partial t} = \frac{\partial \tau_{ij}}{\partial x_j} - \frac{\partial p}{\partial x_i} + \frac{\partial}{\partial x_j}\left(\mu\frac{\partial u_i}{\partial x_j}\right) \tag{16}$$

The fluctuating stress τ_{ij} is expressed as:

$$\tau_{ij} = -\rho\overline{u_i' u_j'} \tag{17}$$

2.3. Turbulence Modeling Using DES

The DES is a hybrid technique that seamlessly integrates RANS modeling with a unified set of equations to represent the resulting flow field [17]. Introduced in 1997, its initial method entails a simple modification of the wall-normal distance scale in Spalart-Allmaras turbulence framework. The core principle of DES is the creation of a combined RANS-LES approach, based on the RANS framework initially formulated by Spalart and Allmaras, with a particular emphasis on turbulent viscosity.

To transition the model toward LES characteristics, Spalart reinterprets the wall-normal d. To preserve this inequality, the turbulent viscosity must be reduced. This is achieved by increasing the dissipation of the parameter, which is accomplished by shortening the length scale. The modified length scale, represented as $\tilde{d}$, is described as:

$$\tilde{d} = \min\left(d, C_{des}\Delta\right) \tag{19}$$

where:

$$\Delta = \max(\Delta x, \Delta y, \Delta z) \tag{20}$$

$$C_{des} = 0.65 \tag{21}$$

The value of C_{des} was determined through a study examining the behavior of decaying isotropic turbulence. Standard LES models encounter difficulties, particularly within the boundary layer regions. The innovative DES approach, developed as a hybrid model [17], effectively combines the strengths of RANS approaches near the boundary layer with Large Eddy Simulation characteristics in regions farther from this layer. This unified solution allows DES to emulate RANS behavior in close proximity to the boundary layer, facilitated by a modified distance function, while adopting Large Eddy Simulation characteristics beyond this region, deviating from the behavior of the Smagorinsky model.

The DES model's behavior closely resembles that of a RANS model near the boundary layer, thanks to the modified distance function, and diverges from this layer by adopting LES characteristics. The applicability of turbulence models with well-defined turbulence length scales, such as the localized Spalart-Allmaras (SA) model, is notable in the DES approach. Conversely, models like the Baldwin-Barth, similar to the SA model but featuring global damping functions, are not recommended for DES due to their less localized nature [17].

2.4. Optimal Selection of Turbulence Models: Comparative Analysis of LES, DES, and RANS

Selecting the appropriate turbulence model in Computational Fluid Dynamics (CFD) simulations is a crucial decision that impacts accuracy, computational cost, and performance efficiency. The choice between LES, DES, and RANS depends on the goals of the analysis, the desired fidelity of transient interactions, and the available computational resources. RANS remains a popular choice due to its computational efficiency and simplicity, averaging flow quantities into mean and fluctuating components. While RANS provides quick and robust results, it often sacrifices transient details, making it less suitable for capturing complex flow interactions, such as vortex shedding or localized boundary layer

developments. However, its widespread availability in commercial CFD tools and ability to handle large-scale aerodynamic studies make it a reliable choice for many applications in aerospace and automotive engineering.

In contrast, the LES model focuses on resolving large-scale turbulent structures explicitly, while smaller scales are modeled. LES offers superior accuracy for transient and unsteady flows, capturing intricate interactions near surfaces and within boundary layers. Although it delivers detailed insights into transient interactions, LES comes at a high computational cost, requiring fine mesh resolution across large domains. This makes it ideal for scenarios where transient interactions are critical, such as airflow around airfoils in high-fidelity aerodynamic studies. Meanwhile, the DES model serves as a hybrid approach, combining the strengths of RANS and LES. It uses RANS in regions where turbulence remains steady and LES in areas with significant transient interactions, striking a balance between computational efficiency and accuracy. DES reduces the cost compared to full LES simulations while still offering good transient resolution and robust performance in complex aerodynamic interactions, such as transonic flows around aircraft wings.

When comparing these models, each has its trade-offs in terms of computational cost, speed, and accuracy. RANS is fast and cost-effective but lacks detailed transient interactions. LES provides high accuracy but at substantial computational expense. DES offers a hybrid approach that ensures a good balance between cost and accuracy. The choice of turbulence model also depends on the specific application, Reynolds number, and Mach number of the flow scenario. RANS is suitable for steady-state simulations and large-scale aerodynamic designs, while LES excels in high-fidelity interactions where transient effects are critical. DES finds a middle ground for complex aerodynamic interactions requiring a seamless blend of local and global interactions.

The integration of turbulence models in CFD workflows typically begins with setting up the geometry and meshing the domain, ensuring an appropriate balance between mesh resolution and computational cost. The solver then processes the equations while incorporating relevant physical models to simulate the desired interactions. In practical terms, engineers must weigh their objectives against computational constraints, choosing the model that offers the best trade-off between simulation speed, accuracy, and cost.

Table 1. Comparative table of turbulence models

Attribute	RANS	LES	DES
Computational Cost	Low	High	Medium
Accuracy	Moderate	High	High
Transient Interaction	Poor	Excellent	Good
Mesh Resolution Needs	Coarse	Fine	Medium
Application Suitability	Steady-State Analysis, Large-Scale Design	High-Fidelity Transient Flows	Hybrid Applications, Transonic
Typical Reynolds Number	High	Varies	Varies
Physical Model Approach	Time-Averaged Quantities	Large-Scale Explicit Resolution	Hybrid Model (RANS + LES)

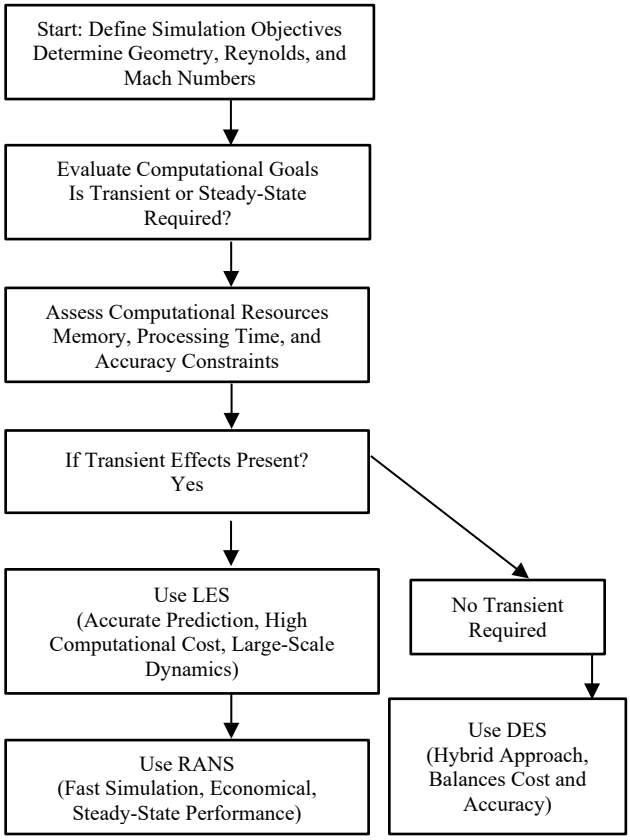

Figure 1. Flowchart of selection of turbulence models

In conclusion, the selection of a turbulence model whether RANS, LES, or DES-depends on the specific requirements of the CFD simulation and the trade-offs between computational demand and accuracy. RANS remains a go to choose for quick, cost-effective analyses, LES delivers detailed transient interactions at higher costs, and DES provides a robust hybrid approach. A thorough understanding of these models enables more informed decisions in aerodynamic design, performance optimization, and predictive accuracy, ensuring the development of efficient and reliable simulations in complex aerodynamic environments across aerospace, automotive, and industrial applications.

3. NUMERICAL ANALYSIS AND DISCUSSION

3.1. Geometric Representation

The NACA Research Center at Langley embarked on an extensive airfoil research program in the 1920s, initiating wind tunnel tests that spanned from 1927 onwards. Subsequently, they compiled a comprehensive catalog featuring 78 distinct airfoils, each uniquely identified by a four-digit code that encapsulates its specific geometric characteristics. The NACA 0012 airfoil features a symmetric design, with the number 12 indicating that its peak thickness is 12% of the wing's chord length.

This investigation is centered on unraveling the intricacies of the aerodynamics associated with the airfoil NACA 0012 within the context of transonic flow. Notably, a discernible shock is observed close to the mid-chord on the top surface of the wing, with the chord length

specifically set at 1 meter. The detailed examination of airflow around this specific airfoil is meticulously conducted at an angle of attack of 1.55°. These analyses are performed within an airflow testing tunnel, maintaining a freestream condition at Mach 0.7. The geometric intricacies of the wing are vividly depicted in Figure 2, providing a visual reference for conducted study.

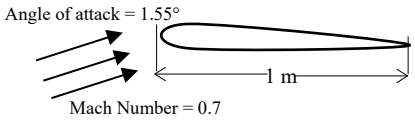

Figure 2. Problem statement [18]

3.2. Borders of Simulation: Exploring Boundary Conditions

The initial step in the numerical simulation process involves creating and adapting the mesh around the airfoil profile. The quality of the mesh is paramount to obtain acceptable and usable results, facilitating the derivation of meaningful conclusions. For this simulation, a structured quadrilateral mesh has been constructed, as illustrated in Figure 3, with over 40,000 cells for Computational Fluid Dynamics computations. While this approach ensures a precise representation of airflow around the wing, it may become inefficient and resource-heavy when applied to more complex geometries.

It is crucial to emphasize that mesh design is a critical step in the simulation process, directly influencing the accuracy of the obtained results. It represents a trade-off between mesh quality and geometric complexity, requiring careful evaluation to ensure result validity in realistic scenarios. Optimizing this step contributes to a more accurate and efficient simulation, despite potential challenges associated with the complexity of considered geometric shapes.

In our study, we've opted for a *C* mesh, a widely employed mesh configuration for simulating airflow around airfoils. This choice is based on the effectiveness of *C* meshes in capturing the aerodynamic features of the geometry. Before commencing the simulation, it is crucial to meticulously plan the boundary conditions to accurately represent the real-world scenario.

For the system input, we define the incoming velocity with an incidence angle of 1.55° and a Mach value of 0.7, aligning with the specific requirements outlined in the problem statement. Given the compressibility of the flow, the total temperature of the free stream is set at 284 K, matching the ambient temperature. Moreover, the viscosity is specified as 1.7894×10^{-5}, while the density is set to 1.225.

Further downstream, a gauge pressure of 0 is assumed, reflecting an open boundary condition. The airfoil itself is treated as a solid wall, considering its physical properties. This comprehensive set of boundary conditions ensures a realistic representation of the external influences on the airfoil and the resulting flow patterns. The visual depiction of these carefully planned boundary conditions is presented in detail in Figure 3, allowing for a clear understanding of their implementation in simulation setup.

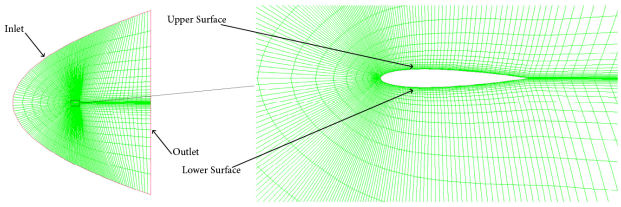

Figure 3. Mesh configuration and boundary conditions [18]

3.3. Validation

In the realm of aerodynamic flow simulation, the validation of objects holds paramount importance as it establishes a foundation for consistency and repeatability in both the implementation and utilization of models. The primary objective of aerodynamic model validation is to rigorously assess the model's ability to accurately replicate physical phenomena by contrasting CFD simulation results with experimental data. In our endeavor for comparison, we turned to the extensive dataset within the project "Experimental Data Collection for Computational Analysis (AGARD-AR-138, 1979)". This dataset encompasses aerodynamic parameters measured on straight wings, ensuring that the sections of these wings remain consistent throughout their entire span. This deliberate choice of profiles serves purpose of subjecting different calculation methods to rigorous testing.

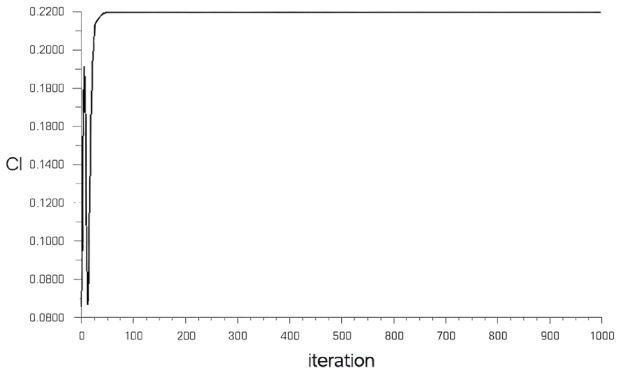

Figure 4. C_l Variations for Mach 0.7 [18]

To enhance the reliability of our validation process, we specifically drew upon aerodynamic data obtained from a variety of wind tunnels. Notably, the wind tunnel tests conducted at the Harris wind tunnel, including those in the Langley Transonic Wind Tunnel (8-Foot), as recommended by Holst [19], were prioritized. This meticulous selection ensures a robust validation process, strengthening the correlation between our CFD simulation results and the benchmark experimental data. By aligning our outcomes with well-established experimental parameters, we enhance the accuracy and credibility of our aerodynamic model.

Table 2. Comparison of (C_d) and (C_l) between numerical and experimental data [18]

	Experimental Data	Numerical Data
Lift Coefficient	0.24100	0.23900
Drag Coefficient	0.00790	0.00810

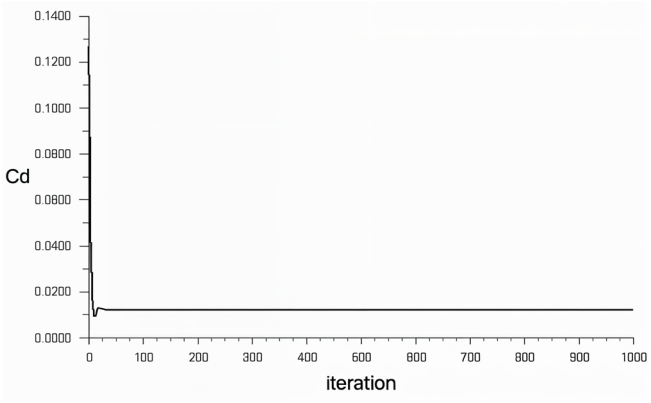

Figure 5. C_d variations for Mach 0.7 [18]

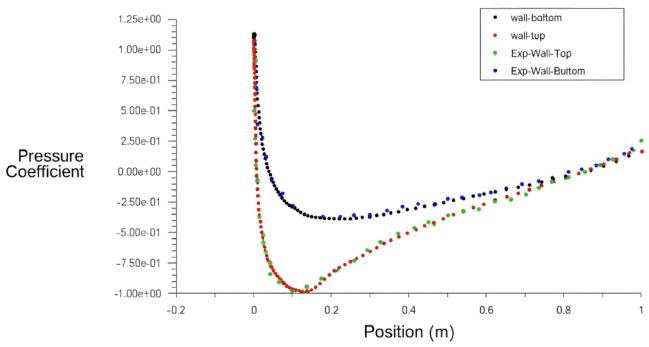

Figure 6. Pressure coefficient (C_p) distribution across wing surfaces at Mach 0.7 [18]

The computational analysis was performed at a Reynolds number of 9×10^6, using a robust implicit solver, with validation achieved through detailed comparisons against experimental data. A critical aspect of this validation involved assessing the C_p, defined as:

$$C_p = \frac{p - p_\infty}{\frac{1}{2}\rho_\infty U_\infty^2} \tag{22}$$

where, ρ_∞ is the static density, U_∞ is the flow velocity at infinity and P_∞ is the static pressure, As well as the drag lift coefficients, which represent the aerodynamic behavior of the wing.

This coefficient is a fundamental metric that provides insights into the aerodynamic performance of the airfoil, specifically its lift and drag characteristics. The computed C_p distributions, depicted in Figure 6, were compared with those obtained from the Harris experiments [20] and NASA's experimental data for both the upper and lower surfaces of the airfoil. The computed C_p distributions, depicted in Figure 6, were compared with those obtained from the Harris experiments [20] and NASA's experimental data for both the upper and lower surfaces of the airfoil.

This comparison demonstrated strong agreement, validating the numerical model's accuracy and its capability to predict aerodynamic behavior reliably. To strengthen the validation process, statistical analysis was employed, including error metrics such as the Root Mean Square Error (RMSE) and the Mean Absolute Percentage Error (MAPE). These metrics quantified deviations between simulated and experimental data, providing a clearer assessment of the simulation's accuracy. Confidence intervals were also calculated to express the statistical reliability of aerodynamic quantities like the pressure coefficient, lift, and drag coefficients, ensuring that discrepancies remained within acceptable bounds.

The lift and drag coefficients, which quantify the aerodynamic forces acting on the airfoil, were analyzed at Mach 0.7 and are presented in Figures 4 and 5, respectively. These coefficients further supported the validation process by highlighting the simulation's ability to replicate experimental aerodynamic performance accurately. Table 2 consolidates the C_l and C_d values obtained from Fluent simulations and NASA experiments, with the observed close agreement reinforcing the reliability of the numerical approach. These results align with the findings reported by Holst [19], who emphasized the importance of precise numerical simulations in capturing aerodynamic drag under transonic conditions.

The graphical representation of C_p distributions allowed for a deeper understanding of the flow behavior around the airfoil, including pressure variations critical to aerodynamic efficiency. This process was supported by the turbulence modeling approach, which incorporated advanced techniques such as the Baldwin-Barth turbulence model [21]. Incorporating visual comparisons and clear annotations enhanced the interpretation of results, while also serving as a foundation for practical applications in airfoil optimization. Error metrics like RMSE and MAPE provided a quantitative measure of the fidelity of CFD simulations against experimental results, ensuring that the predictive models were accurate and reliable.

Additionally, flow visualizations, such as streamlines and vortex structures, established a direct link between numerical predictions and the underlying aerodynamic phenomena, offering more intuitive insights. A sensitivity analysis examining the effects of mesh refinement and turbulence model selection further strengthened the validation by identifying key factors that influence the simulation's accuracy and performance. Such analyses ensured that the computational model remained robust and adaptable to various aerodynamic conditions and design constraints.

By integrating these statistical comparisons and visual analyses, the validation framework became not only a benchmarking tool for comparing numerical models with experimental data but also a comprehensive methodology for refining CFD simulation predictions. This rigorous validation underscores the capability of the computational approach to capture complex aerodynamic interactions accurately, providing a reliable foundation for applications in airfoil design, aerospace engineering, and industrial applications, where precision and performance are crucial.

3.4. Comparison

The integration of a RANS-based turbulence model within the DES framework prioritizes the lowest value between the turbulent length scale and the maximum grid size, enabling a seamless adaptation between LES and

RANS approaches. This adaptive behavior is particularly evident in simulations involving solid walls, where the model transitions smoothly to RANS-type turbulence modeling. In contrast, in regions away from the wall, LES dominates, capturing unsteady and large-scale turbulent structures effectively. The computational results, illustrated through the C_p distribution in Figure 7 and the comparison of C_l and C_d values in Table 3, highlight the effectiveness of the Spalart-Allmaras model in both RANS and DES formulations. While DES proves advantageous for capturing transient features, the LES approach requires significantly higher computational resources and finer meshing near the wall to achieve similar accuracy.

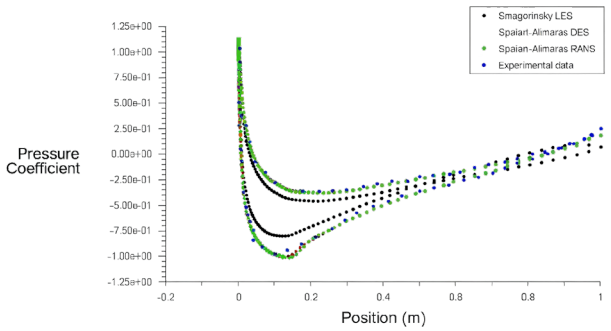

Figure 7. C_p distribution of LES, RANS and DES models and experimental data over NACA 0012 airfoil [23]

Table 3. Comparison of (C_d) and (C_l) between numerical and experimental data

	Experimental Data	SA RANS	DES	LES
C_L	0.241	0.234	0.239	0.073
C_D	0.0079	0.0117	0.0112	0.0133

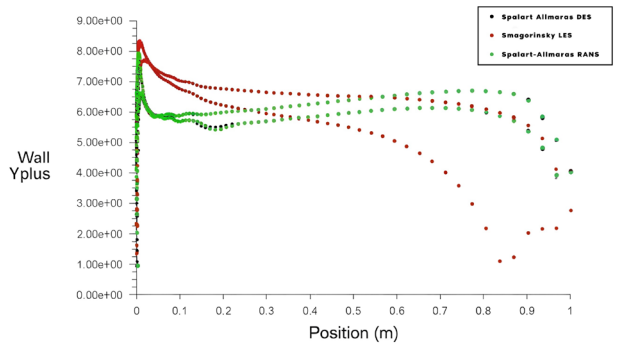

Figure 8. Comparison of Y^+ for RANS, DES and LES turbulence models near the boundary layer

A critical aspect of these simulations is the distribution of $y+$, a dimensionless wall distance that governs near-wall turbulence modeling, as illustrated in Figure 8. In this study, $y+$ values ranged from 1 to 9, an ideal range for LES or DNS simulations, ensuring a fine resolution of the boundary layer and accurate representation of turbulence near the wall. This fine resolution significantly impacts key flow characteristics, including lift, drag, and pressure profiles. The strong correlation between the $y+$ distributions and experimental observations reinforces the robustness of the computational model and its alignment with real-world aerodynamic phenomena. The analysis underscores the importance of mesh refinement strategies and turbulence model selection, as these directly influence the accuracy of simulations in capturing boundary layer behavior and transonic flow features.

The study also highlights the trade-offs inherent in turbulence model selection. DES, while effective in capturing unsteady flow features, imposes substantial computational demands, making its widespread use in industrial applications challenging. On the other hand, RANS models, though computationally efficient, lack the capability to resolve transient and small-scale turbulence phenomena. The Smagorinsky model within the LES framework offers detailed insights into boundary layer dynamics, particularly around critical regions like the trailing edge of the wing, but necessitates ultra-fine meshing to minimize errors. These findings emphasize the critical role of meshing strategies and the careful consideration required when selecting turbulence models for specific aerodynamic applications.

From a practical perspective, the study provides valuable guidance for aircraft designers, enabling them to select the optimal turbulence model based on their specific design requirements. The balanced integration of RANS and DES formulations facilitates fast and efficient simulations, offering a trade-off between computational cost and accuracy. This approach ensures reliable predictions of aerodynamic performance while optimizing time and resources—a crucial consideration for complex simulations around aircraft profiles.

Moreover, the insights from turbulence models have significant real-world implications. For instance, the DES model's ability to capture transient aerodynamic effects can directly improve aircraft wing design, enhancing lift and drag performance, which results in better fuel efficiency and reduced operational costs. In wind energy applications, selecting the appropriate model allows engineers to optimize turbine blade shapes, ensuring higher energy output and operational stability by accurately predicting aerodynamic forces under changing wind conditions. Industrial applications also benefit from enhanced design flexibility, where choosing DES over LES or RANS enables better decision-making in scenarios requiring high fidelity simulations of transonic flows, boundary layer interactions, and unsteady aerodynamic effects.

For transonic aerodynamic simulations, model selection should balance accuracy and computational cost. The hybrid DES model effectively combines LES and RANS, capturing unsteady flow details while maintaining efficiency. LES provides high-resolution near-wall interactions but demands significant computational resources. In contrast, RANS models offer quick and cost-effective simulations, suitable for steady-state analyses. Engineers should choose the turbulence model based on design objectives, considering factors like flow complexity, resource availability, and the need for transient or steady-state accuracy. By addressing these specific aerodynamic challenges with the appropriate turbulence modeling approach, industries can achieve a

more efficient balance between simulation accuracy, computational resources, and cost, paving the way for more advanced and resource-effective engineering solutions.

To further enhance this study, an artificial intelligence (AI)-based perspective can be incorporated to automate and optimize turbulence model selection. Machine learning techniques, such as neural networks and reinforcement learning, could analyze historical simulation data and recommend appropriate turbulence models based on the configuration and flow conditions. This AI-driven approach would not only improve prediction accuracy but also significantly reduce computation time, making simulations faster and more efficient. In particular, the integration of AI could streamline decision-making for engineers, automating the selection process for turbulence models and optimizing aircraft wing configurations. By adopting a comprehensive methodology that combines advanced turbulence modeling techniques, mesh refinement strategies, and AI-driven optimization, this study contributes to enhancing simulation accuracy and efficiency. It also underscores the importance of ongoing research to refine turbulence modeling approaches, ensuring their applicability to real-world aerodynamic challenges while addressing the computational demands of modern engineering applications.

4. CONCLUSIONS

This study analyzed the flow around the NACA airfoil using ANSYS/FLUENT, comparing simulation results with experimental data under Mach 0.7 and Reynolds numbers near 9 million. The hybrid DES model proved effective by combining LES for external flow interactions with RANS near the boundary layer, balancing accuracy and computational efficiency. This model offers practical benefits for aircraft wing design, improving lift and drag performance while reducing fuel costs.

The Smagorinsky model within LES accurately captured small vortices near walls but required dense meshing in the boundary layer. These trade-offs highlight the importance of mesh strategies and computational resources in aerodynamic design. The findings are also relevant for wind turbine optimization, where selecting the right model enhances energy efficiency and performance. Integrating artificial intelligence could further optimize turbulence model selection, reducing computation time and improving design decisions. In summary, choosing the appropriate turbulence model, combined with AI-driven tools, enables more efficient and cost-effective simulations, ensuring better performance predictions in aerospace and renewable energy applications.

NOMENCLATURES

1. Acronyms

DES	Detached Eddy Simulation
LES	Large Eddy Simulation
RANS	Reynolds-Averaged Navier-Stokes
CFD	Computational Fluid Dynamics
DNS	Direct Numerical Simulation
SGS	Subgrid Scale model
V2C	Vortex to Circulation Profile
SA	Spalart-Allmaras Model
Cl	Lift Coefficient
Cd	Drag Coefficient
Cp	Pressure Coefficient

2. Symbols / Parameters

u_i' : The portion of the strain rate tensor

$\overline{S}_{ij}$: The strain rate tensor associated with resolved scale

ν_t : The turbulent viscosity

$\tilde{d}$: The updated length scales

τ_{ij} : The Reynolds stresses

ρ_∞ : The static density

U_∞ : The flow velocity at infinity

P_∞ : The static pressure

y^+ : Non-dimensional wall distance

REFERENCES

[1] J. Tu, G. Yeoh, C. Liu, Y. Tao, "Computational Fluid Dynamics: A Practical Approach", Elsevier, Technical and Multiphysics Reliability Systems, Issue 1, Vol. 1, No. 1, pp. 1-350, Amsterdam, Netherlands, 2023.

[2] J.S. Shang, "Computational Fluid Dynamics Application to Aerospace Science", The Aeronautical Journal, Issue 113, Vol. 113, No. 5, pp. 619-632, London, UK, 2009.

[3] A. Dorri, K. Dhoska, M. Alcani, M. Baco, "Computational Simulation of Heat Transfer Through Fins of Different Shapes in an Air-Cooled Internal Combustion Engine", International Journal on Technical and Physical Problems of Engineering, (IJTPE), Issue 54, Vol. 15, No. 1, pp. 248-254, Tehran, Iran, March 2023.

[4] J. Garcia, E. Bilbao, O. Bravo, C. Gonzalez, M. Varela, P. Rodriguez, "Blade Aerodynamic Design and Analysis as First Step to Achieve the Expected Power Performance of a Small Wind Turbine", Nuclear Energy, Issue 10, Vol. 10, No. 2, pp. 12-40, Madrid, Spain, 2015.

[5] T.J. Jamaleddine, M.B. Ray, "Application of Computational Fluid Dynamics for Simulation of Drying Processes: A Review", Drying Technology, Issue 28, Vol. 28, No. 2, pp. 120-154, New York, USA, 2010.

[6] F.O. Echavarri, E. Zulueta, J.A. Ramos Hernanz, J.M. Lopez Guede, J.M. Larranaga Lesaka, "Particle Swarm Optimization Based Tuning for a Small Wind Turbine Pitch Control", International Journal on Technical and Physical Problems of Engineering (IJTPE), Issue 1, Vol. 10, No. 4, pp. 101-120, Bilbao, Spain, 2015.

[7] A. Nayir, E. Rosolowski, L. Jedut, "New Trends in Wind Energy Modeling and Wind Turbine Control", International Journal on Technical and Physical Problems of Engineering (IJTPE), Issue 4, Vol. 2, No. 3, pp. 51-59, Istanbul, Turkey, September 2010.

[8] H. Ashley, W.P. Rodden, "Wing-Body Aerodynamic Interaction", Annual Review of Fluid Mechanics, Issue 4, Vol. 4, No. 1, pp. 431-472, San Francisco, USA, 1972.

[9] D.C. Wilcox, Turbulence Modeling for CFD, DCW Industries, Technical Guide, Los Angeles, USA, 1998.
[10] O. Reynolds, "An Experimental Investigation of the Circumstances Which Determine Whether the Motion of Water Shall Be Direct or Sinuous, and of the Law of Resistance in Parallel Channels", Proceedings of the Royal Society of London, Issue 35, Vol. 35, No. 1, pp. 84-99, London, UK, 1883.
[11] S. Jones, "Investigations of the NACA 0012 Airfoil at Low Reynolds Numbers", Journal of Fluid Mechanics, Issue 25, Vol. 25, No. 4, pp. 123-150, Cambridge, UK, 2010.
[12] S. Jones, "The Influence of Airfoil Geometry on the Separation Bubble Dynamics at Low Reynolds Numbers", Journal of Fluid Mechanics, Issue 650, Vol. 650, No. 6, pp. 197-223, Boston, USA, 2010.
[13] S. Schmidt, F. Thiele, "Detached Eddy Simulation of Flow Around an Airfoil", Flow, Turbulence, and Combustion, Issue 71, Vol. 71, No. 3, pp. 261-278, Hannover, Germany, 2003.
[14] L. Zhu, W. Zhang, J. Kou, Y. Liu, "Machine Learning Methods for Turbulence Modeling in Subsonic Flows Around Airfoils", Physics of Fluids, Issue 31, Vol. 31, No. 5, pp. 015-105, Paris, France, 2019.
[15] P. Apalart, S. Allmaras, "A One-Equation Turbulence Model for Aerodynamic Flows", 30th Aerospace Sciences Meeting, Conference Proceedings, No. 439, Dayton, Ohio, USA, 1992.
[16] M. Shur, P. Spalart, M. Strelets, A. Travin, "Detached-Eddy Simulation of an Airfoil at High Angle of Attack", Engineering Turbulence Modelling and Experiments, pp. 669-678, 1999.
[17] R. El Maani, S. Elouardi, B. Radi, A. El Hami, "Multiobjective Aerodynamic Shape Optimization of NACA0012 Airfoil Based Mesh Morphing", International Journal for Simulation and Multidisciplinary Design Optimization, Vol. 11, pp. 11, 2020.
[18] T. Coakley, "Numerical Simulation of Viscous Transonic Airfoil Flows", 25th AIAA Aerospace Sciences Meeting, No. 416, 1987.
[19] T.L. Holst, "Computational Fluid Dynamics Drag Prediction: Results from the Viscous Transonic Airfoil Workshop", Tech, Rep, 1988.
[20] C.D. Harris, "Two-Dimensional Aerodynamic Characteristics of the NACA 0012 Airfoil in the Langley 8-Foot Transonic Pressure Tunnel", Tech. Rep, 1981.
[21] U.C. Goldberg, S.V. Ramakrishnan, "Pointwise Version of Baldwin-Barth Turbulence Model", International Journal of Computational Fluid Dynamics, Vol. 1, pp. 321-338, 1993.
[22] S. Elouardi, B. Radi, R. El Maani, L. Zahiri, "Comparison of Turbulence Approaches Modelling the Flow Around the NACA 0012 Profile", 3rd International Conference on Innovative Research in Applied Science, Engineering and Technology, IEEE, pp. 1-6, May 2023.

BIOGRAPHIES

Name: **Soufiane**
Surname: **El Ouardi**
Birthday: 28.09.1986
Birthplace: Casablanca, Morocco
Bachelor: Mechanical Engineering, Mechanical Engineering, FST Settat, Hassan I University, Settat, Morocco, 2010
Master: Mechanical Engineering, Mechanical Engineering, ENSET Rabat, Mohammed V University, Rabat, Morocco, 2012
Doctorate: Mechanical Engineering, Mechanical Engineering, FST Settat, Hassan I University, Settat, Morocco, 2021
The Last Scientific Position: Prof., Department of Mechanics, Higher Normal School of Technical Education (ENSET), Hassan II University, Casablanca, Morocco, Since 2021
Research Interests: Fluid Mechanics, Vibrations, Optimization, Structural Analysis and Materials
Scientific Publications: 3 Papers

Name: **Bouchaib**
Surname: **Radi**
Birthday: 06.01.1963
Birthplace: Casablanca, Morocco
Bachelor: Applied Mathematics, Mathematics Department, FS Ain Chok, Hassan II University, Casablanca, Morocco, 1986
Master: Mathematics and Applications, Mathematics Department, FS Besancon, Franche-Comte University, Besancon, France, 1988
Doctorate: Engineering Science, Mathematics Department, Franche-Comte University, Besancon, France, 1992
The Last Scientific Position: Prof., Technic Department, FST Settat, University Hassan First, Settat, Morocco, Since 2010
Research Interests: Applied Mechanics, Applied Mechanics
Scientific Publications: 30 Papers, 10 Books, 4 Projects, 10 Theses
Scientific Memberships: Manufacturing Scientific Society

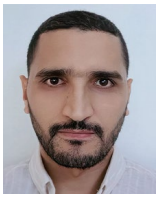

Name: **Rabii**
Surname: **El Maani**
Birthday: 09.06.1988
Birthplace: Casablanca, Morocco
Bachelor: Mechanic Engineering, Department, Faculty, Hassan I University, Settat, Morocco, 2000
Master: Mechanic Engineering, Hassan I University, Settat, Morocco, 2011
Doctorate: Mechanic engineering, Hassan I University, Settat, Morocco, 2016

The Last Scientific Position: Prof., ENSA Khouribga, University Sultan Moulay Slimane, Khouribga, Morocco, Since 2018
Research Interests: Mechanical Engineering, Reliability, Optimization,
Scientific Publications: 10 Papers, 1 Thesis

Name: **Jaouad**
Surname: **Smily**
Birthday: 28.04.1986
Birthplace: Marrakesh, Morocco
Bachelor: Civil Engineering, Mohammadia School of Engineers, Rabat, Morocco, 2009
Engineering Diploma: Mechanics, Department of Physics, Faculty of Sciences, Mohammed V University, Rabat, 1996
Doctorate: FST Settat, Hassan I University, Settat, Morocco, 2024
The Last Scientific Position: Prof., Mohammed VI School of Training in Building and Public Works, Settat, Morocco, Since 2013
Research Interests: Fluid Mechanics, Civil Engineering, Optimization, Structural Mechanics

Name: **Laidi**
Surname: **Zahiri**
Birthday: 01.01.1963
Birthplace: Benslimane, Morocco
Bachelor: Mechanical Engineering, ENSET, Mohammed V University, Rabat, Morocco, 1987
Master: Mechanics, Department of Physics, Faculty of Sciences, Mohammed V University, Rabat, Morocco, 1996
Doctorate: Mechanical Engineering, SSDIA Laboratory, Faculty of Science and Technology (FST), Hassan II University, Mohammedia, Morocco, 2018
The Last Scientific Position: Prof., ENSET Mohammedia, Hassan II University of Casablanca, Mohammedia, Morocco, Since 1996
Research Interests: Mechanical Engineering, Innovative Materials, Structural Analysis
Scientific Publications: 453 Papers, 10 Books, 3 Projects, 40 Theses

Name: **Khalifa**
Surname: **Mansouri**
Birthday: 20.05.1968
Birthplace: Azilal, Morocco
Bachelor: Computer Science, ENSET, Hassan II University of Casablanca, Mohammedia, Morocco, 1991
Master: CEA (Computer Science), ENSET, Hassan II University of Casablanca, Mohammedia, Morocco, 1992
Doctorate: Calculation and Optimization of Structures, Mohammed V University, Rabat, Morocco, 1994
HDR (Habilitation): Computer Science, Hassan II University, Casablanca, Morocco, 2010
Doctorate (Second): Computer Science, Hassan II University, Casablanca, Morocco, 2016
The Last Scientific Position: Prof., Computer Science and Researcher, Director of the M2S2I Research Laboratory, Department of Computer Science, ENSET, Hassan II University, Casablanca, Morocco, Since 2016
Research Interests: Information Systems, E-Learning Systems, Real-Time Systems, Artificial Intelligence,
Scientific Publications: 453 Papers, 10 Books, 3 Projects, 40 Theses
Scientific Memberships: Member Modeling Optimization Numerical of the Moroccan Association of Computer Scientists, IEEE, ACM (Computation)